Soils and Rocks
An International Journal of Geotechnical and Geoenvironmental Engineering
www.soilsandrocks.com
ISSN 1980-9743
ISSN-e 2675-5475

Contribution to the numerical modelling analysis of displacements caused by tunnel construction in discontinuous rock masses: a case study of Boukhadra iron mine (Algeria)

Ali Hamdane[1,2#], Mekki Mellas[1], Zied Benghazi[2], Adel Djellali[2]

Case Study

Keywords
Tunnel stability
Rock masses
Geomechanical classifications
Failure strength
Regression analysis
Numerical modelling

Abstract

This paper presents a comprehensive study of the stability conditions of a rock mass surrounding a tunnel, using numerical modelling analysis of displacements induced by tunnel construction. The case study focuses on the Boukhadra iron ore mine in Algeria. This research employs empirical equations from literature based on geomechanical classifications to provide the most appropriate geotechnical input data for simulation. In addition to those equations, a novel correlation equation relating the rock mass ratio (*RMR*) and the rock quality index (*Q*) was developed. This equation gives a high regression coefficient, revealing a strong correlation (R^2) of 0.878. It provides a better estimation of the rock mass characteristics: Young's moduli (E), Poisson's ratio (ν), cohesion (c), and friction angle (φ), compared to the existing literature-based correlation equations. The estimated parameters were used to pass from a discontinuous medium to a continuous equivalent, making numerical modelling using finite element method easier. Compared with intact rock and direct equations, the numerical simulation results based on the new equation fit well with the in-situ observations, with predicted displacements remaining within the same order of magnitude as observed deformations, providing more reliable understanding of rock mass behaviour. The new equation proposed in this paper provides a substantial evaluation of the rock mass parameters required for the design process of underground structures when used within their respect acceptable ranges.

1. Introduction

Tunnel construction in discontinuous rock masses poses significant geotechnical challenges due to complex geological conditions, which often lead to instability. Accurate numerical modelling is essential for assessing hazards and ensuring the safety of underground structures. While traditional geotechnical analysis relied on empirical methods, recent technological advancements have made numerical methods more accessible (Stille & Palmström, 2008). However, the safety of underground openings remains closely tied to the design process (Bieniawski, 1984; Palmström & Stille, 2007; Hudson, 2012; Xing et al., 2017; Abdellah et al., 2018; Hezaimia et al., 2019; Chaoui et al., 2025).

Numerical methods like the Finite Element Method, Boundary Element Method, and Discrete Element Method are central to simulating rock mass behaviour (Bieniawski, 1973; Barton et al., 1974; Wang et al., 2023). Discontinuities in rock masses impact the choice of modelling approaches, which may treat the rock mass as either a continuous or discontinuous medium (Scheldt, 2002; Ferrero et al., 2004; Maazallahi & Majdi, 2021; Boukarm et al., 2024). Continuous models, such as the Finite Element Method, are often preferred for hard rock analysis due to the challenges of modelling jointed rock masses (Brown, 1987).

Accurate geotechnical characterisation is critical, and requires reliable strength and deformability parameters (Driouch et al., 2021; Benghazi et al., 2025), which can be time-consuming, costly, and sometimes un reliable (Rahman & Sarkar, 2021). Therefore, these parameters are often estimated using empirical relationships based on classification systems (Hoek & Diederichs, 2006; Salimi et al., 2016; Oliveira & Lima, 2020). Classification systems like the rock mass ratio (*RMR*) and the Geological Strength Index (*GSI*) provide essential input data for estimating rock mass properties (Hoek, 1994; Hoek & Brown, 1997; Hoek et al., 1998, 2000; Marinos & Carter, 2018; Somodi et al., 2021; Benghazi et al., 2025). Combining these systems enhances reliability in rock engineering, as demonstrated by Palmström (1995) and Bieniawski (1989).

[#]Corresponding author. E-mail address: hamdane.ali@univ-biskra.dz
[1]Mohammed Khider University, Department of Civil Engineering and Hydraulics, Biskra, Algeria.
[2]Echahid Larbi Tebessi University - Tebessa, Department of Mining and Geotechnology, Tebessa, Algeria.
Submitted on December 21, 2025; Final Acceptance on April 22, 2026; Discussion open until November 30, 2026.
Editor: Renato P. Cunha

https://doi.org/10.28927/SR.2026.020325

Several correlations between the Rock Mass Rating (*RMR*) and the rock quality index (*Q*) have been proposed, notably by Bieniawski (1976) and Jethwa et al. (1982). However, these relationships were derived from heterogeneous international datasets and may be less reliable for site-specific geological conditions.

This study provides two significant contributions to the fields of rock mass characterization and tunnel engineering. It uses intact rock parameters to estimate the rock mass properties, employing Hoek-Brown equations and *RMR* values to assess the failure strength of the rock mass surrounding an underground opening.

A total of 53 geomechanical observations were collected along the tunnel alignment. Observation points were selected to cover the different lithological units. The sampling strategy combined systematic spacing along the alignment with targeted measurements at zones of geological interest, such as contacts between lithologies or areas showing visible structural features. At each location, measurements were taken from the tunnel walls where accessible. This approach ensures that the dataset captures both the spatial variability and the key structural features of the rock mass, providing a representative basis for calculating *RMR* and Q parameters from field discontinuity mapping.

First, a new empirical correlation between *RMR* and Q is developed using data collected from the various lithological units of the Boukhadra iron mine (north east Algeria). The proposed equation is calibrated on site-specific lithological units, providing a more refined and accurate estimate of rock mass properties (R1-1).

The second contribution lies in the application and validation of this new correlation within numerical models for tunnel stability analysis. The predicted geomechanical parameters obtained from the new equation are compared with those derived from intact rock properties and from conventional empirical relations.

Furthermore, three modelling approaches were compared using intact rock parameters, empirical equations, and the proposed RMR-Q correlation to evaluate the geomechanical behaviour of the Boukhadra mine tunnel using finite element analysis in Plaxis 2D. The finite element simulations reveal that the new equation yields displacement patterns that are not only consistent with theoretical expectations but also better reflect the degrading influence of discontinuities on the rock mass behaviour. This enhances its relevance for practical engineering design in similar geological contexts.

Integrating intact rock parameters with empirical equations and classification systems provides a comprehensive and robust approach to estimating rock mass properties, which is crucial for ensuring the stability and safety of underground openings.

2. Site description

The study area is located in the Boukhadra iron ore mine in eastern Algeria, about 45 km north of Tebessa (Figure 1). The site lies between longitudes 8°01’30”–8°03’18” and latitudes 35°45’54”–35°44’42”. Previous investigations of the Boukhadra mining district have highlighted the complexity of the structural framework and its influence on rock mass behaviour (Benyoucef et al., 2022, 2023). The central geological structure consists mainly of Triassic marls, dolomite, limestone, and sandstone; Aptian sandstone and limestone; and Tertiary polygenic conglomerates with a carbonate matrix and interbedded sandstone (Kerbati et al., 2020).

The study tunnel (situated at an altitude of 1105 m) is above the groundwater level, with a section area of 13 m^2 and an approximate length of 250 m. This underground opening passes through several sub-vertical sedimentary formations, including limestone, iron ore, sandstone, conglomerate, mineralised marl, multicoloured marl, and yellow marl (Gadri et al., 2012).

3. Methodology

3.1 Characterisation of the different formations

The geotechnical characterisation of appropriate ground parameters of the mine’s rock mass was performed from field observations and laboratory tests (Table 1). Based on Young’s moduli and unconfined compressive strength values, it can be observed that the stiffness of the iron ore, limestone, sandstone, and the mineralised marl ranges from stiff to extremely stiff, and the strength ranges from medium to very high. In contrast, the stiffness of the yellow marl, the conglomerate, and the multicoloured marl ranges from poorly to moderately stiff. Their strength ranges from very low to low, according to the French Tunnelling and Underground Space Association (AFTES, 2003).

3.2 Failure strength of the rock mass surrounding the tunnel

The *GSI* is used to demonstrate the mechanical behaviour of the rock masses and their engineering qualities (Somodi et al., 2018). Engineers use the GSI/Hoek-Brown criterion extensively as a basis for modelling different structures in rock masses (Marinos & Carter, 2018).

3.3 Geomechanical classification

Different classification methods were applied to estimate the geotechnical quality of rock formations, including the RMR system (Bieniawski, 1989), the Q-system (Barton et al., 1974), and RMi (Palmström, 1995). The RMR system and the Q-system are the most widely used in tunnel studies worldwide. The Q-system can often be determined faster during tunnelling or drilling investigations, because it relies mainly on geological observations and core logging.

Based on Table 2, the results of the Q-system fit more with those of the rock mass index (*RMi*) system than those of the RMR system. However, in general, the three systems are in

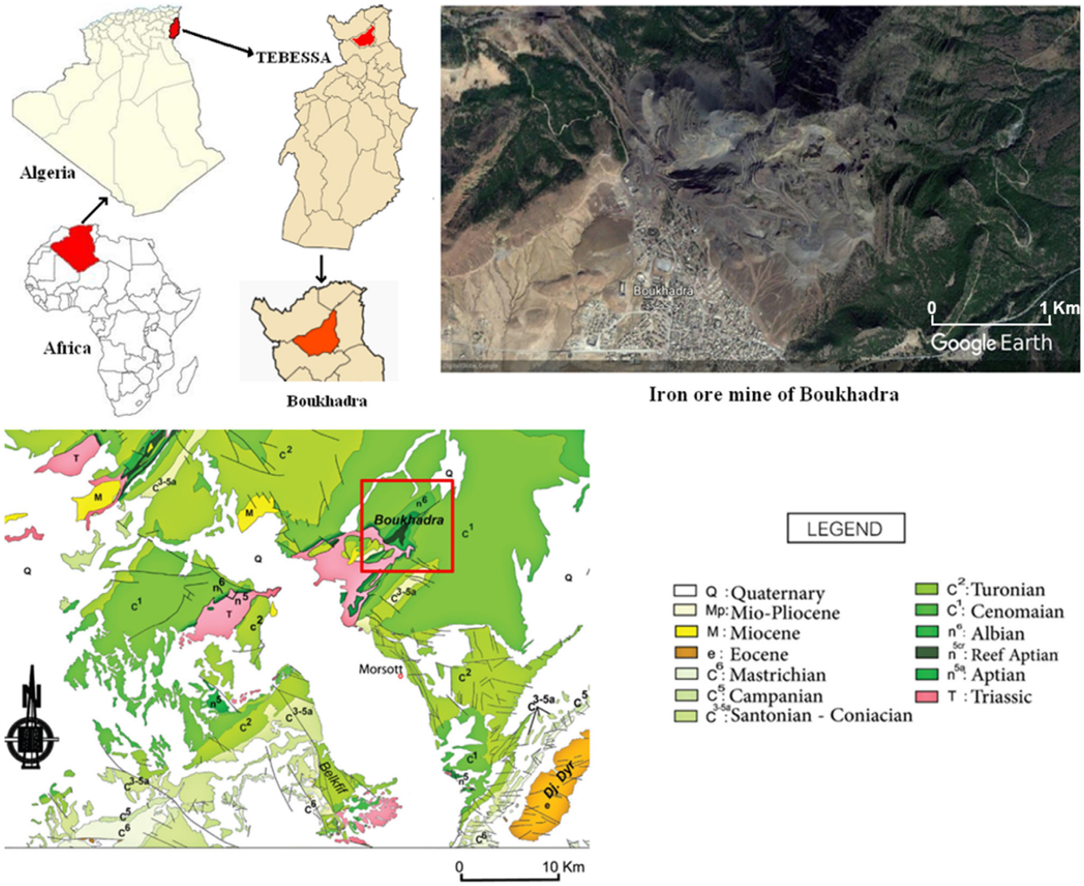

Figure 1. Situation and Geological map of Bokhadra iron mine, after Bakelli et al. (2022).

Table 1. Geotechnical characteristics and description of the different formations (intact rocks) according to the AFTES (2003).

	Internal friction (°)	Unite weight (kN/m³)	Cohesion (MPa)	Unconfined Compressive Strength (MPa)	Stiffness description	Young's modulus (GPa)	Strength description	Poisson's ratio
Limestone	37.76	26	3.65	60	extremely stiff	42	very high strength	0.22
Iron ore	49.59	27	8.56	71	very stiff	63.9	high strength	0.25
Sandstone	44.37	23	4.53	50	stiff	13.75	medium strength	0.35
Conglomerate	11.90	22	0.56	5	stiff	1.75	medium strength	0.35
Mineralised marl	29.14	24	2.19	30	moderately stiff	6.00	low strength	0.30
Multicoloured marl	8.02	19.5	0.40	5	moderately stiff	0.75	very low strength	0.38
Yellow marl	17.86	22	1.11	9	poorly stiff	1.80	very low strength	0.33

Table 2. Results of the classification systems applied to the different geological formations.

Formations	*RMR*		*Q*		*RMi*	
	Value	quality	Value	quality	Value	quality
Limestone	50	Fair	15.05	Good	1.56	high
Iron ore	70	Good	21	Good	2.34	high
Sandstone	59	Fair	19.6	Good	1.55	high
Conglomerate	19	Very Poor	3.5	Poor	0.09	low
Mineralised marl	44	Fair	14	Good	0.75	Moderate
Multicolored marl	29	Poor	9.85	Fair	0.11	Moderate
Yellow marl	39	Poor	12.95	Good	0.21	Moderate

good agreement concerning the rocks' qualities. The obtained qualities confirm the findings of the previous results (yellow marl, the conglomerate, and the multicoloured marl are the least resistant and constitute an imminent geotechnical risk).

3.4 Correlation analysis

To overcome this difficulty, a correlation equation specific to the Boukhadra mine condition linking the *Q* value to the *RMR* value would be very advantageous. To achieve this objective, a correlation study based on data collected from different geological formations was conducted.

The selected correlation model is logarithmic. This choice is justified because the *Q*-index spans several orders of magnitude (≈0.001-1000), as it is defined as the product of several discontinuity-related factors, resulting in a highly skewed distribution. Applying the natural logarithm to *Q* reduces skewness and yields a relationship more compatible with the roughly linear scale of *RMR* (Laderian & Abaspoor, 2012). Consequently, many empirical RMR-Q correlations reported in the literature adopt a logarithmic form, as it better represents the non-linear relationship between the two indices and typically provides an improved statistical fit (higher R^2 and better residual behaviour). Therefore, the use of logarithmic regression for the RMR-Q correlation is both methodologically justified and consistent with common practice in rock mass classification studies (Ghimire et al., 2025).

The resulting correlation illustrates a logarithmic relationship between *RMR* and *Q* values, with a very good coefficient of determination $R^2 = 0.878$ (McNeill, 2001). It shows a clear tendency for *RMR* to increase with *Q* (Figure 2).

The high regression coefficient indicates a strong correlation between *RMR* and *Q*, allowing the estimation of one value from the other. The obtained Equation 1 defines this relationship:

$$RMR = 6.248 \ln Q + 42.71 + \varepsilon \quad (1)$$

The statistical robustness of the proposed correlation was evaluated using residual analysis and significance testing (Table 3). Residuals were computed as the difference between observed and predicted *RMR* values and showed a mean close to zero with no systematic trend across the *Q* range, indicating the absence of bias. The regression yielded a root mean square error (*RMSE*) of approximately 2.25 *RMR* units. The estimated coefficients were statistically significant, with *p-values* lower than 0.001. The 95% confidence intervals (*CI*) were 5.41-7.09 for the slope and 41.00-44.42 for the intercept, confirming the reliability of the proposed RMR-Q relationship.

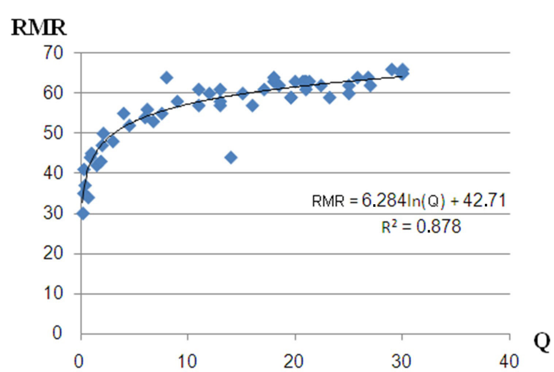

Figure 2. Logarithmic correlation between *RMR* and Q.

3.5 Validation of the developed equation

Many users apply this proposal to determine the output of one classification system from another using correlation equations. The commonly used equation correlating the RMR system to the Q-system is shown in Figure 3.

It can be noted that the range of inaccuracy is about ± 50% or more, which may consequently lead to incorrect decisions. Also, the two systems have different limitations, and the Q-system applies a logarithmic scale, which may impose additional errors (Palmström, 2009).

The obtained correlation equation shows a good agreement with the common correlation. It represents a low level of inaccuracy (Figure 3), especially when $RMR \geq 30$.

To further evaluate the predictive performance of the proposed equation, it was compared with classical correlations developed by Bieniawski (1989) and Palmström (2009) using statistical error metrics. The comparison was carried out using Root Mean Square Error (*RMSE*), Mean Absolute Error (*MAE*), and Mean Absolute Percentage Error (*MAPE*) indicators based on the collected dataset. The results are summarised in Table 4. The proposed equation exhibits significantly lower prediction errors ($RMSE = 2.43$; $MAE = 1.80$; $MAPE = 3.50\%$) compared with the Bieniawski and Palmström correlations, which show *RMSE* values of 8.01 and 7.64, respectively.

These results indicate that the proposed correlation provides a substantially improved prediction of *RMR* for the

Table 3. Regression results for statistical validation of the proposed correlation.

Parameter	Estimate	Std. Error	*t-value*	*p-value*	95% *CI*
intercept	42.71	0.85	50.2	<0.001	41.00-44.42
ln(*Q*) coefficient	6.248	0.42	14.9	<0.001	5.41-7.09

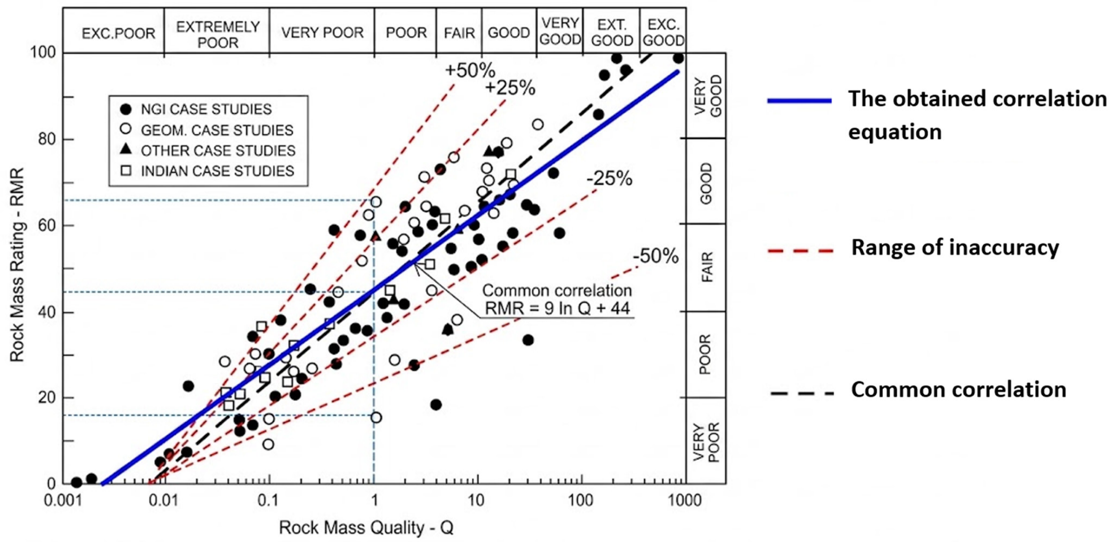

Figure 3. Correlation between the *RMR* and the *Q*-index with deviation from the common correlation after Bieniawski (1976) and Jethwa et al. (1982) (Palmström, 2009).

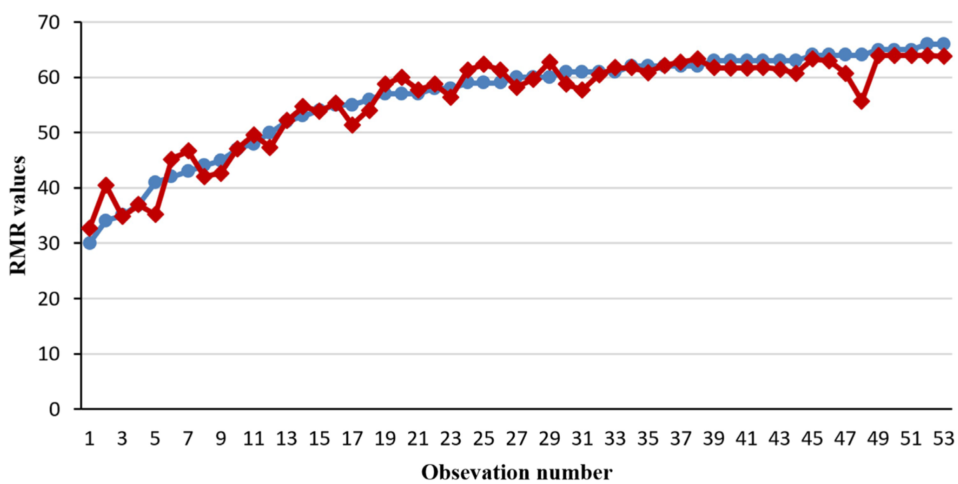

Figure 4. Observed versus predicted values of *RMR*.

Table 4. Statistical comparison of RMR-Q correlations.

Correlation	*RMSE*	*MAE*	*MAPE*
The new developed equation	2.43	1.80	3.50
Bieniawski (1989)	8.01	7.29	12.68
Palmström (2009)	7.64	7.27	13.62

Boukhadra rock mass conditions, likely due to its calibration using local geological and geomechanical data.

3.6 Determination of mechanical characteristics using the developed equation

For each geological formation, both the directly determined *RMR* values and the corresponding *Q* values derived from the correlation were used to estimate the mechanical parameters required for numerical modelling. The obtained parameters, based on the new equation, show a good agreement between the quality of the massif (based on the *RMR*) given by this equation and with the direct application of the *RMR* system for the first three formations (Limestone, Iron ore, and sandstone), in addition to mineralised marl (Figure 4). The geotechnical characteristics of the built models are presented in Table 5.

3.7 Stability analysis by numerical simulation

Table 6 presents the commonly used direct relations of rock mass classifications and the most needed rock mass parameters. However, the results obtained from these equations are highly divergent, with differences exceeding 100% for the same geological formation. This divergence indicates that the numerical simulation results obtained using these values as input could be inconsistent and do not represent the behaviour of the rock mass. To address this issue, a selection of the data to be used must be made based on the non-contradiction with the values of the intact rock parameters, as presented previously in Table 1.

3.8 Numerical modelling

To validate the proposed approach, the numerical results obtained using the newly developed equation were compared with those derived from intact rock parameters and from empirical relations reported in the literature. Accordingly, three numerical models were established for each formation using PLAXIS 2D to assess the effect of the

Table 5. Geotechnical characteristics used in numerical modelling.

Formations	Modelling conditions	Internal friction (°)	Unite width (kN/m³)	Cohesion (MPa)	Young's modulus (GPa)	Poisson's ratio
Limestone	Intact rocks	37.76	26	3.65	42.00	0.22
	Direct relations	29.40	26	0.96	10.00	0.33
	Equation 1	49.82	26	0.86	17.43	0.32
Iron ore	Intact rocks	49.59	27	8.56	63.90	0.25
	Direct relations	36.92	27	1.83	31.62	0.26
	Equation 1	50.86	27	2.03	19.64	0.32
Sandstone	Intact rocks	44.37	23	4.53	13.75	0.35
	Direct relations	31.69	23	1.16	16.79	0.30
	Equation 1	50.65	23	1.15	19.16	0.32
Mineralised marl	Intact rocks	29.14	24	2.19	6.00	0.30
	Direct relations	23.36	24	0.41	7.08	0.41
	Equation 1	49.60	24	0.34	16.98	0.32

Table 6. Direct relations of rock mass classifications and rock mass parameters (Aydan et al., 2014).

Property of the rock mass	Empirical relation	Proposed by
Deformation modulus, E_{rm} (GPa)	$E_{rm} = 10^{\left(\frac{RMR-10}{10}\right)}$	Serafim & Pereira (1983)
	$E_{rm} = 25\log Q\,(\text{GPa})$	Grimstad & Barton (1993)
Friction angle, φ_m (°)	$\varphi_m = 20\sigma_{cm}^{0.2}$	Aydan et al. (1993)
	$\varphi_m = 20 + 0.5RMR$	Aydan & Kawamoto (2001)
Cohesion, c_m (MPa)	$c_m = \frac{\sigma_{cm}}{2}\frac{1-sin\varphi_m}{cos\varphi_m}$	Aydan & Kawamoto (2001)
	$c_m = \left(\frac{RQD}{J_n}\times\frac{1}{SRF}\times\frac{\sigma_{ci}}{100}\right)$	Barton (2002)
Poisson's ratio, ν_m	$\nu_m = 0.25\left(1+e^{\sigma_m/4}\right)$	Aydan et al. (1993)
	$\nu_m = 0.5-0.2\frac{RMR}{RMR+0.2\left(100-RMR\right)}$	Tokashiki & Aydan (2010)

E_{rm} deformation modulus of rock mass, *RMR* rock mass rating, Q rock mass quality, σ_{ci} uniaxial compressive strength of intact rock, σ_{cm} uniaxial compressive strength of rock mass, *RQD* Rock Quality Designation, φ_m friction angle of rock mass, c_m cohesion of rock mass, ν_m Poisson's ratio of rock mass, J_n joint set rating, *SRF* stress reduction factor.

geotechnical characteristics determination method on the obtained results. These models are numerical ones based on rock mass characteristics obtained from direct relations, and from Equation 1, respectively.

3.8.1 Geometry and boundary conditions

Figure 5 presents the geometry and boundary conditions of the mine's tunnel and the built models. The tunnel section considered in this study has an average height h of 3.5 m and an average width l of 4.0 m, leading to a typical cross-sectional area S of about 12 to 13 m^2. The tunnel is set at varying depths H depending on the geological formation: 150 m in limestone, 135 m in iron-ore strata, 75 m in sandstone, and 124 m in mineralised marl. For numerical modelling, a model width L of 50 m was employed to represent the rock mass surrounding the tunnel excavation. The adopted model width-to-tunnel width ratio, L/l = 12.5, aims to achieve zero displacement at the boundaries (Mestat, 2002).

The vertical stress (σ_v) was assumed to result from the self-weight of the overlying rock mass. The horizontal stress (σ_h) was automatically computed in PLAXIS 2D using the at-rest earth pressure coefficient K_0, according to the relation presented in Equation 2:

$$\sigma_h = K_0 \times \sigma_v \qquad (2)$$

where the K_0 values were determined based on the Poisson's ratio of the rock mass for each geological formation (v_m), as follows in Equation 3:

$$K_0 = \frac{v_m}{1 - v_m} \qquad (3)$$

The finite element mesh was generated using a medium-density triangular mesh for the global model geometry. Local mesh refinement was applied around the excavation in order to improve calculation accuracy while maintaining reasonable computational time.

Displacements were extracted from the numerical model along predefined profiles around the excavation. Vertical displacements above the roof and below the floor were obtained along horizontal profiles located at distances of 0, 0.5, 1, 1.5, 2, and 2.5 m from the excavation boundary. In contrast, horizontal displacements were obtained along a vertical profile located at the same distances from the excavation sidewall.

3.8.2 Constitutive law and behaviour analysis

Complex behaviour laws require the measurement of a large number of parameters that only some projects will justify, or the available technical means do not allow for obtaining these data. Thus, in 90% of cases, the elastoplastic laws of Mohr-Coulomb (five parameters) or Hoek and Brown (six parameters) are used (Chalhoub & Pouya, 2006).

Although the Hoek-Brown criterion provides a more realistic representation of rock mass failure, the Mohr-Coulomb model was adopted for the numerical simulations due to its simplicity, fewer required parameters, and widespread use in practical engineering analyses (Labuz & Zang, 2012; Li et al., 2024). The Hoek-Brown parameters obtained from RocLab were converted into equivalent Mohr-Coulomb parameters over the relevant stress range, allowing the nonlinear failure envelope to be approximated by a linear criterion suitable for PLAXIS simulations. In tunnel studies, the Mohr-Coulomb law is highly reliable for analysing the surrounding rock mass, typically in drained conditions (Mestat, 2002). The two-dimensional (2D) model, calculated as a plane strain

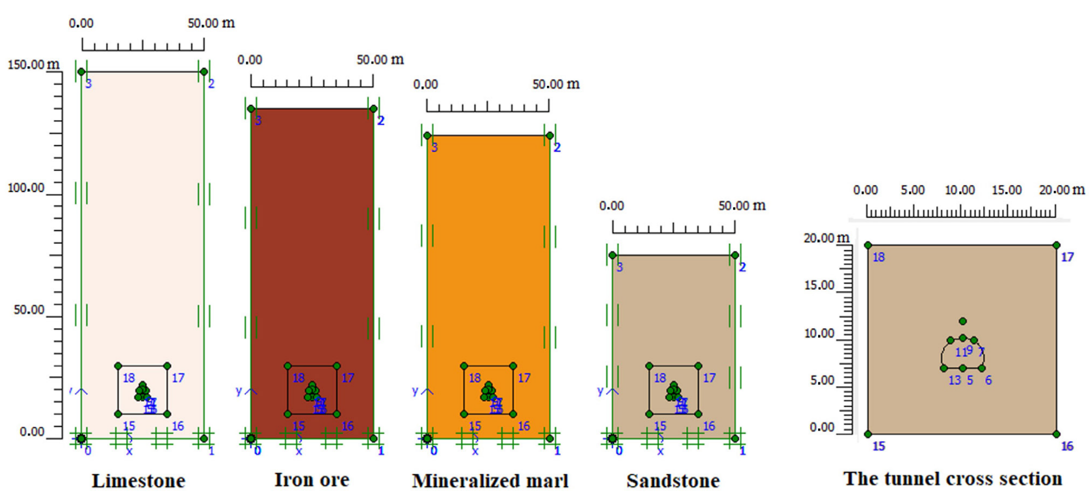

Figure 5. Numerical model geometries for the different rock formations and the tunnel cross-section.

in the tunnel's cross-section, accounts for 98% of the numerical calculations performed at design offices (Mauldon & Goodman, 1990).

4. Results and discussion

4.1 Strength analysis and geomechanical classification

The Hoek-Brown failure criterion was used to estimate the rock mass strength parameters from intact rock properties. The input parameters consisted of the uniaxial compressive strength of the rock mass (σ_{cm}), the material constant m_i, the Geological Strength Index (*GSI*), and the disturbance factor *D* (Table 7). These parameters were processed using RocLab 1.0 (RocScience, 2014) to determine the Hoek-Brown rock mass constants. Since numerical modelling was performed using the Mohr-Coulomb constitutive model, the Hoek-Brown envelope was converted to equivalent Mohr-Coulomb parameters (cohesion *c* and friction angle *φ*) by fitting a linear approximation over the relevant confining stress range (Figure 6).

The analysis identifies three strength groups: (1) iron ore, the strongest; (2) sandstone, limestone, and mineralised marl; and (3) yellow marl, conglomerate, and multicoloured marl, the weakest. This last group represents a significant geotechnical hazard, where the majority of on-site observed instabilities occur, reflecting their high brittleness and low cohesion and highlighting the importance of formation-specific support measures (Zheng et al., 2023). These results emphasise that relying solely on intact rock properties would underestimate risks in weaker formations, whereas converting to Mohr-Coulomb parameters enables practical implementation in numerical simulations (Vučemilović, 2022). The classification is consistent with the observed behaviour of rock masses in stratified tunnel projects, reinforcing the validity of combining Hoek-Brown estimates with empirical classification (Hoek et al., 2000).

4.2 Numerical modelling results

The computed displacements in the vertical and horizontal directions for selected nodes, using the finite element package PLAXIS v.2012, for each geological formation of the studied tunnel, are presented graphically in Figures 7 to 9.

A comparative analysis of the three modelling approaches: intact rock parameters, empirical direct relations, and the proposed RMR-Q correlation (Equation 1), highlights their influence on the predicted tunnel response. The model based on intact rock properties systematically produces the smallest displacement values because it neglects the weakening effects of discontinuities such as joints and bedding planes. However, the mechanical behaviour of rock masses is strongly controlled by structural anisotropy associated with these features (Saroglou et al., 2018; Gong et al., 2024). For example, the maximum roof displacements predicted using intact rock parameters range from 0.53×10^{-3} mm to 0.76×10^{-3} mm, depending on the formation. In contrast, the numerical results from empirical direct relations yield intermediate displacement values, increasing to between 1.08×10^{-3} mm and 1.50×10^{-3} mm, corresponding to an increase of approximately 97-104% compared with the intact rock model and reflecting the reduced stiffness of the rock mass. However, these displacements still exhibit noticeable variability, reflecting the dispersion associated with empirical equations derived from heterogeneous datasets. The model using Equation 1 consistently predicts larger displacements around the excavation, reaching up to 2.67×10^{-3} mm in limestone and 2.51×10^{-3} mm in mineralised marl. In relative terms, the proposed correlation increases the predicted displacements by approximately 214-256% compared with intact rock parameters and by about 60-80% relative to empirical direct relations. This behaviour can be explained by the fact that the proposed correlation implicitly captures rock mass anisotropy through parameters embedded in the Q and RMR classification systems (such as joint orientation, spacing, and condition) thereby providing more representative rock mass properties for the numerical modelling of discontinuous rock masses.

Table 7. Hoek-Brown criterion characteristics of the different geological formations.

Formations	Geological Strength Index (*GSI*)	m_i	Disturbance factor (*D*)	Deformation modulus E_{rm} (GPa)	Unconfined Compressive Strength of the rock mass σ_{rm} (MPa)
Limestone	46	09	0.8	3.00	4.67
Iron ore	64	12	0.8	13.76	11.61
Sandstone	51	17	0.8	1.34	6.30
Conglomerate	14	21	0.8	0.04	0.15
Mineralised marl	38	10	0.8	0.28	1.86
Multicolored marl	21	5	0.8	0.02	0.10
Yellow marl	33	9	0.8	0.07	0.44

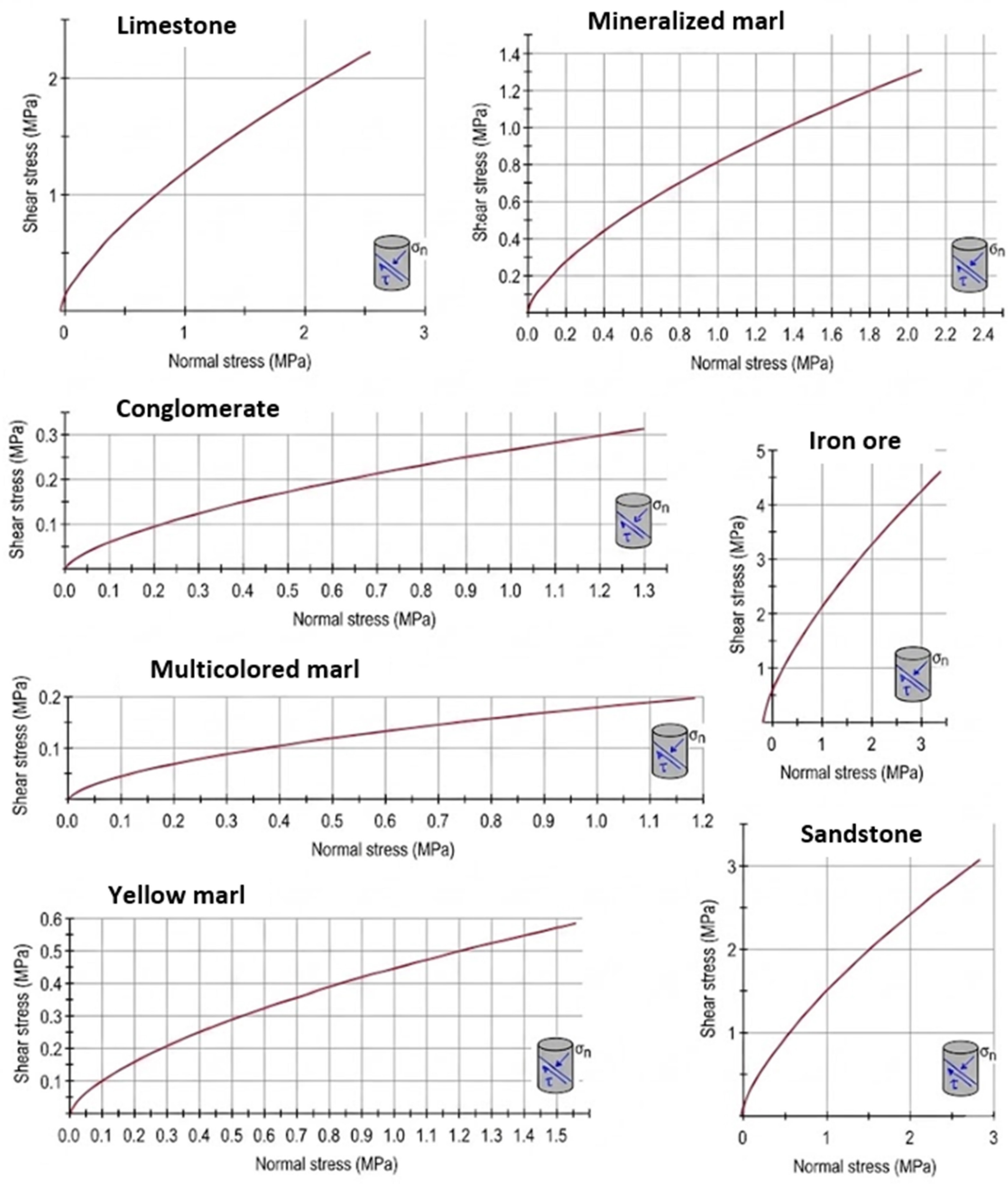

Figure 6. Results of rock strength analysis.

Notably, displacements decrease sharply beyond the first meter from the excavation face, reflecting the varying stiffness and strength of each formation. Strong formations (iron ore, sandstone) exhibit self-supporting behaviour, while weaker formations (yellow marl, conglomerate) undergo greater deformations, confirming the geomechanical classification.

The predicted displacements are consistent with those reported in similar tunnel excavation studies in jointed rock masses, typically ranging from a few millimetres to several centimetres depending on rock mass quality and tunnel depth (e.g., Xing et al., 2017; Boukarm et al., 2024). This agreement supports the realism of the modelling results.

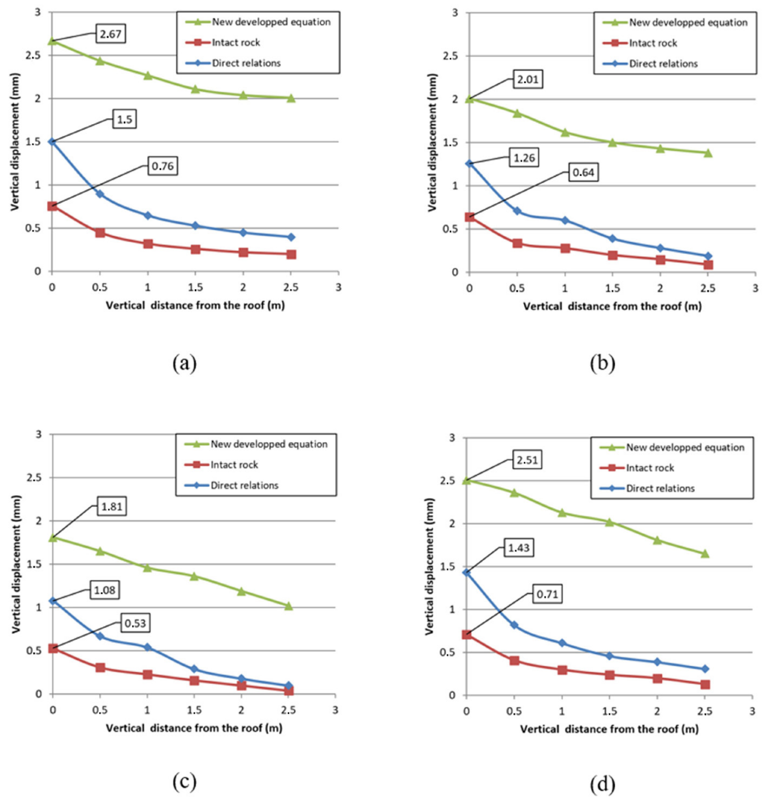

Figure 7. Vertical displacement from the roof with maximum values indicated at the excavation boundary: (a) limestone; (b) iron ore; (c) sandstone; (d) mineralised marl.

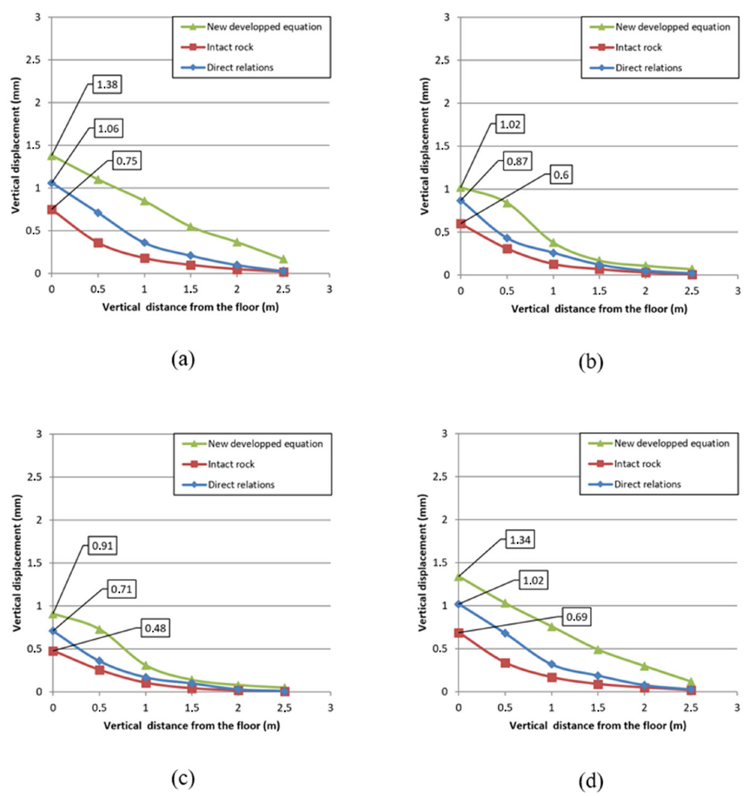

Figure 8. Vertical displacement from the floor with maximum values indicated at the excavation boundary: (a) limestone; (b) iron ore; (c) sandstone; (d) mineralised marl.

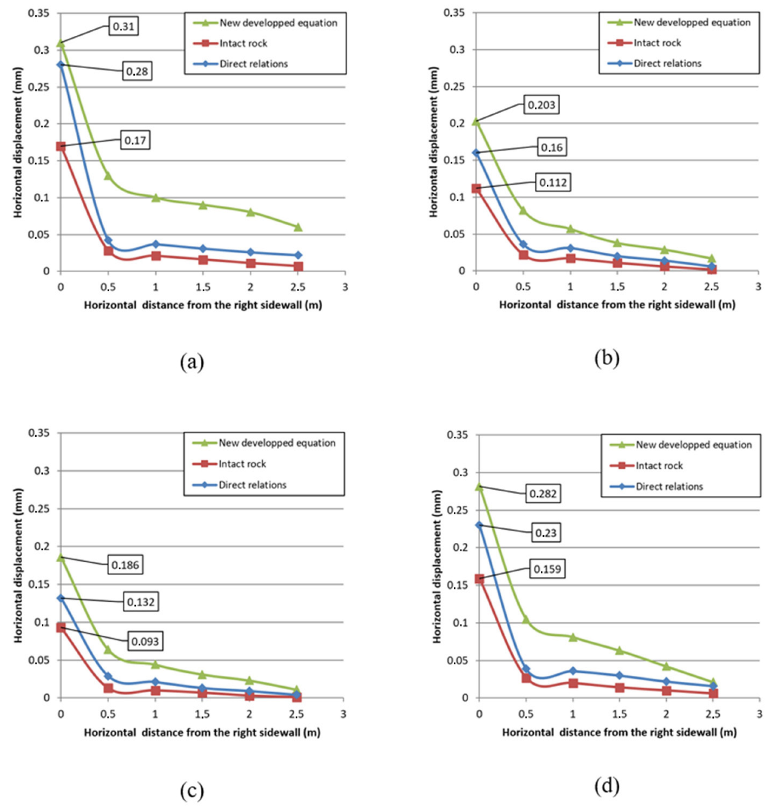

Figure 9. Horizontal displacement from the right sidewall with maximum values indicated at the excavation boundary: (a) limestone; (b) iron ore; (c) sandstone; (d) mineralised marl.

5. Conclusion

This work presents a significant contribution to the numerical modelling analysis of displacements caused by tunnel construction in rock masses using various methods. The research findings affirm that the new developed equation for rock mass characterisation is effective and provides a mechanically consistent representation of the complex geological conditions at the Boukhadra underground iron mine, compared with existing methods.

The predictive equation's correlation coefficient for *RMR* is 87.80%, exceeding those of existing RMR-Q relationships in the literature, which are known to produce large deviations, often exceeding ±50%, indicating the developed model's reliability for rock masses within the range of rock masses represented in the dataset, corresponding approximately to *RMR* values between 30 and 70 and to sedimentary lithologies similar to those encountered in the Boukhadra mining district.

The proposed correlation shows a strong statistical relationship (R^2 = 0.878). The regression analysis also shows low prediction errors (*RMSE* = 2.43, *MAE* = 1.80, and *MAPE* = 3.50%), demonstrating a significant improvement compared with commonly used correlations reported in the literature. These results confirm that calibrating empirical relationships using site-specific geological data improves the reliability of rock mass characterisation.

The proposed RMR-Q correlation consistently predicts larger deformation values, increasing the estimated roof displacement by approximately 60-80% relative to empirical direct relations and by more than 200% compared with intact rock models, depending on the geological formation. This behaviour reflects the stronger influence of discontinuities captured by the proposed correlation. It highlights the importance of using appropriate rock mass characterisation methods for realistic numerical modelling of underground excavations.

A vital partnership between these systems and numerical methods, such as the finite element and finite difference methods, is imperative to guarantee the most refined conception of medium behaviour.

While this study provides a strong numerical framework based on empirical rock mass characterization, the absence of real-time displacement monitoring limits the immediate calibration of the model. However, the consistency between proposed numerical results and observed rock mass behavior in the studied site and similar stratified formations supports the model's preliminary validity.

Declaration of interest

The authors have no conflicts of interest to declare. All co-authors have observed and affirmed the contents of the paper and there is no financial interest to report.

Authors' contributions

Ali Hamdane: conceptualization, investigation, data curation, visualization, writing – original draft, writing – review & editing. Mekki Mellas: conceptualization, methodology, supervision, project administration. Zied Benghazi: conceptualization, data curation, methodology, validation, writing – original draft, writing – review & editing. Adel Djellali: validation, writing – review & editing.

Data availability

All data produced or examined in the course of the current study are included in this article.

Declaration of use of generative artificial intelligence

This work was prepared with the assistance of generative artificial intelligence (GenAI) [Chat Gpt] with the aim of improving the clarity of certain parts of the manuscript. The entire process of using this tool was supervised, reviewed and when necessary edited by the authors. The authors assume full responsibility for the content of the publication that involved the aid of GenAI.

List of symbols and abbreviations

c	Cohesion
c_m	Cohesion of the rock mass
h	Tunnel average height
l	Tunnel average width
m_i	Hoek-Brown material constant for intact rock
p-value	Probability value
AFTES	French Tunnelling and Underground Space Association
CI	Confidence interval
D	Disturbance factor
E	Young's modulus
E_{rm}	Deformation modulus of the rock mass
GSI	Geological Strength Index
H	Tunnel depth in each formation
J_n	Joint set rating
K_0	At-rest earth pressure coefficient
L	Model width
MAE	Mean Absolute Error
MAPE	Mean Absolute Percentage Error
Q	Rock quality index
R^2	Coefficient of determination
RMi	Rock mass index
RMR	Rock mass ratio
RMSE	Root Mean Square Error
RQD	Rock Quality Designation
S	Tunnel section
SRF	Stress Reduction Factor
ε	Residual error
ν	Poisson's ratio
ν_m	Poisson's ratio of the rock mass
σ_h	Horizontal stress
σ_{rm}	Unconfined Compressive Strength of the rock mass
σ_v	Vertical stress
φ_m	Friction angle of the rock mass

References

Abdellah, W.R., Ali, M.A., & Yang, H.-S. (2018). Studying the effect of some parameters on the stability of shallow tunnels. *Journal of Sustainable Mining*, 17(1), 20-33. https://doi.org/10.1016/j.jsm.2018.02.001.

Aydan, Ö., Akagi, T., & Kawamoto, T. (1993). The squeezing potential of rocks around tunnels; theory and prediction. *Rock Mechanics and Rock Engineering*, 26(2), 137-163. https://doi.org/10.1007/BF01023620.

Aydan, Ö., & Kawamoto, T. (2001) The stability assessment of a large underground opening at great depth. In *Proceedings of the 17th international mining congress and exhibition of Turkey (IMCET 2001)* (Vol. 1, pp. 277-288), Ankara, Turkey.

Aydan, Ö., Ulusay, R., & Tokashiki, N. (2014). A new rock mass quality rating system: rock mass quality rating (RMRQ) and its application to the estimation of geomechanical characteristics of rock masses. *Rock Mechanics and Rock Engineering*, 47(4), 1255-1276. https://doi.org/10.1007/s00603-013-0462-z.

Bakelli, A., Sami, L., Boutaleb, A., Kolli, O., Haddouche, O., Demir, Y., & Zedef, V. (2022). Evolution and genesis of fluorite mineralization in the Ouenza region (North-east of Algeria): evidence from fluid inclusions and stable isotopes (C, O, and S). *Arabian Journal of Geosciences*, 15(6), 514. https://doi.org/10.1007/s12517-022-09726-8.

Barton, N., Lien, R., & Lunde, J. (1974). Engineering classification of rock masses for the design of tunnel support. *Rock Mechanics*, 6(4), 189-236. https://doi.org/10.1007/BF01239496.

Barton, N. (2002). Some new Q-value correlations to assist in site characterisation and tunnel design. *International Journal of Rock Mechanics and Mining Sciences*, 39(2), 185-216. https://doi.org/10.1016/S1365-1609(02)00011-4.

Benghazi, Z., Hamdane, A., Djellali, A., Tobal, R., & Makhlouf, B. (2025). Multi-method geotechnical assessment of the 7 september 2022 landslide at Kef Essnoun Phosphate Mine, Algeria. *Geotechnical and Geological Engineering*, 43(1), 17. https://doi.org/10.1007/s10706-024-03027-5.

Benyoucef, A.A., Gadri, L., Hadij, R., Mebrouk, F., & Harkati, E. (2022). Mining operations and geotechnical issues in deep hard rock mining: case of Boukhadra iron mine. *Geomatics, Landmanagement and Landscape*, 4(4), https://doi.org/10.15576/GLL/2022.4.27.

Benyoucef, A.A., Gadri, L., Hadji, R., Slimane, H., Mebrouk, F., & Hamed, Y. (2023). Empirical graphical and numerical model for the schematization of underground mining operations in the heterogeneous rock masses, case of Boukhadra mine, NE Algeria. *Arabian Journal of Geosciences*, 16(3), 165. https://doi.org/10.1007/s12517-023-11219-1.

Bieniawski, Z.T. (1973). Engineering classification of jointed rock masses. *Civil Engineer in South Africa*, 15(12), 335-343.

Bieniawski, Z.T. (1976). Rock mass classification in rock engineering. In Z.T. Bieniawski (Ed.), *Exploration for Rock Engineering – Proceedings of the Symposium* (Vol. 1, pp. 97-106), Cape Town. Rotterdam: A.A. Balkema..

Bieniawski, Z.T. (1984). *Rock mechanics design in mining and tunneling*. Rotterdam: A.A. Balkema.

Bieniawski, Z.T. (1989). *Engineering rock mass classifications*. New York: John Wiley & Sons.

Boukarm, R., Fredj, M., & Saadoun, A. (2024). Performance evaluation of tunnel support system in jointed rock mass by numerical simulation: a case study. *KSCE Journal of Civil Engineering*, 28(4), 1534-1545. https://doi.org/10.1007/s12205-024-0529-2.

Brown, E.T. (1987). *Analytical and computational methods in engineering rock mechanics*. London: Allen & Unwin.

Chalhoub, M., & Pouya, A. (2006). A geometrical approach to estimate the mechanical REV of a fractured rock mass. In *Proceedings of the 1st Euro Mediterranean Conference in Advances on Geomaterials and Structures* (pp. 663-670), Hammamet, Tunisia.

Chaoui, S., Djellali, A., Benghazi, Z., & Debojit, S. (2025). Analytical and numerical stability analysis of underground pillars subjected to shear loading: a case study of the Chaabet El Hamra Zinc Mine, Algeria. *Journal of Mining and Environment*. In press.

Driouch, A., Ouadif, L., & Lahmili, A. (2021). Correlation between Q-System and Rock Mass Rating of the Serpentine Rock Mass at the Bou Azzer Mine in the Central Anti-Atlas of Morocco. *Annals of the Romanian Society for Cell Biology*, 25(6), 12726-12733.

Ferrero, A.M., Migliazza, M., & Giani, G.P. (2004). Analysis of tunnel stability: comparison between continuous and discontinuous approaches. *International Journal of Rock Mechanics and Mining Sciences*, 41, 646-651. https://doi.org/10.1016/j.ijrmms.2004.03.113.

French Tunnelling and Underground Space Association – AFTES. (2003). *GT1R1A1: characterization of rock masses useful for the design and construction of underground structures.* Paris.

Gadri, L., Boumazbeur, A., Nouioua, I., Boukeloul, M.L., Hamdane, A., Mouici, R., Mebrouk, F., & Ibrahim, H. (2012). Study of fractured rock masses deformation in Boukhadra (Tebessa) underground mine empirical and numerical approach (N-E Algeria). *Journal of Geology and Mining Research*, 4(2), 23-34. https://doi.org/10.5897/JGMR11.041.

Ghimire, B., Adhikari, S., & Luitel, P. (2025). Correlation analysis of *RMR* and Q systems in Himalaya Rock Mass conditions: a case study of Seti-khola Hydropower Project, Nepal. *Technical Journal*, 5(1), 13-21. https://doi.org/10.3126/tj.v5i1.86887.

Grimstad, E., & Barton, N. (1993) Updating the Q-system for NMT. In *Proceedings of the International Symposium on Sprayed Concrete - Modern Use of Wet Mix Sprayed Concrete for Underground Support*, Fagernes, Norway. Oslo: Norwegian Concrete Association.

Gong, B., Zhao, T., Thusyanthan, I., & Tang, C. (2024). Modelling rock fracturing by a novel implicit continuous to discontinuous method. *Computers and Geotechnics*, 166, 106035. https://doi.org/10.1016/j.compgeo.2023.106035.

Hezaimia, I., Boukelloul, M.L., Merah, C., Berrah, Y., Hamdane, A., Benghazi, Z., & Kahoul, I. (2019). Selection of new appropriate mining method: case of Boukhadra iron ore mine, NE Algeria. *Arabian Journal of Geosciences*, 12(17), 537. https://doi.org/10.1007/s12517-019-4641-4.

Hoek, E. (1994). Strength of rock and rock masses. *ISRM News Journal*, 2, 4-16.

Hoek, E., & Brown, E.T. (1997). Practical estimates of rock mass strength. *International Journal of Rock Mechanics and Mining Sciences*, 34(8), 1165-1186. https://doi.org/10.1016/S1365-1609(97)80069-X.

Hoek, E., & Diederichs, M.S. (2006). Empirical estimation of rock mass modulus. *International Journal of Rock Mechanics and Mining Sciences*, 43(2), 203-215. https://doi.org/10.1016/j.ijrmms.2005.06.005.

Hoek, E., Kaiser, P.K., & Bawden, W.F. (2000). *Support of underground excavations in hard rock* (1st ed.). Hoboken: CRC Press. https://doi.org/10.1201/b16978.

Hoek, E., Marinos, P., & Benissi, M. (1998). Applicability of the Geological Strength Index (GSI) classification for very weak and sheared rock masses: the case of the Athens Schist Formation. *Bulletin of Engineering Geology and the Environment*, 57(2), 151-160. https://doi.org/10.1007/s100640050031.

Hudson, J.A. (2012). Design methodology for the safety of underground rock engineering. *Journal of Rock Mechanics and Geotechnical Engineering*, 4(3), 205-214. https://doi.org/10.3724/SP.J.1235.2012.00205.

Jethwa, J.L., Dube, A.I.C., Singh, B., Singh, B., & Mithal, R.S. (1982). Evaluation of classification system for tunnels in non-squeezing ground conditions. In W. Wittke (Ed.), *Rock Mechanics: Caverns and Pressure Shafts – Proceedings of the ISRM Symposium* (pp. 607-612). Rotterdam: A.A. Balkema.

Kerbati, N.R., Gadri, L., Hadji, R., Hamad, A., & Boukelloul, M.L. (2020). Graphical and numerical methods for stability analysis in surrounding rock of underground excavations, example of Boukhadra Iron Mine N.E Algeria. *Geotechnical and Geological Engineering*, 38(3), 2725-2733. https://doi.org/10.1007/s10706-019-01181-9.

Labuz, J.F., & Zang, A. (2012). Mohr-Coulomb failure criterion. *Rock Mechanics and Rock Engineering*, 45(6), 975-979. https://doi.org/10.1007/s00603-012-0281-7.

Laderian, A., & Abaspoor, M.A. (2012). The correlation between *RMR* and *Q* systems in parts of Iran. *Tunnelling and Underground Space Technology*, 27(1), 149-158. https://doi.org/10.1016/j.tust.2011.06.001.

Li, W., He, P., Wang, G., Zheng, W., Fan, K., Wang, L., & Zheng, C. (2024). Elastoplastic solution for tunnel composite support structures based on Mohr-Coulomb criterion. *Buildings*, 14(11), 3657. https://doi.org/10.3390/buildings14113657.

Maazallahi, V., & Majdi, M. (2021). Directional rock mass rating (DRMR) for anisotropic rock mass characterization. *Bulletin of Engineering Geology and the Environment*, 80(6), 4471-4499. https://doi.org/10.1007/s10064-021-02143-3.

Marinos, V., & Carter, T.G. (2018). Maintaining geological reality in application of GSI for design of engineering structures in rock. *Engineering Geology*, 239, 282-297. https://doi.org/10.1016/j.enggeo.2018.03.022.

Mauldon, M., & Goodman, R.E. (1990). Rotational kinematics and equilibrium of blocks in a rock mass. *International Journal of Rock Mechanics and Mining Sciences & Geomechanics Abstracts*, 27(4), 291-301. https://doi.org/10.1016/0148-9062(90)90531-6.

McNeill, D. (2001). *Modern statistics.* Sydney: Southwood Press.

Mestat, P. (2002). Application de la base de données MOMIS à la validation du calcul des ouvrages souterrains. *Bulletin des Laboratoires des Ponts et Chaussées*, (236), 9-75.

Oliveira, P.L., & Lima, H.M. (2020). Correlations of rock mass classifications applied to ferruginous caves. *REM - International Engineering Journal*, 73(2), 267-272. https://doi.org/10.1590/0370-44672019730017.

Palmström, A. (1995). *RMi - a rock mass characterization system for rock engineering purposes* [Doctoral thesis]. University of Oslo, Norway.

Palmström, A. (2009). Combining the *RMR*, Q, and RMi classification systems. *Tunnelling and Underground Space Technology*, 24(4), 491-492. https://doi.org/10.1016/j.tust.2008.12.002.

Palmström, A., & Stille, H. (2007). Ground behaviour and rock engineering tools for underground excavations. *Tunnelling and Underground Space Technology*, 22(4), 363-376. https://doi.org/10.1016/j.tust.2006.03.006.

Rahman, T., & Sarkar, K. (2021). Lithological Control on the Estimation of Uniaxial Compressive Strength by the P-Wave Velocity Using Supervised and Unsupervised Learning. *Rock Mechanics and Rock Engineering*, 54(6), 3175-3191. https://doi.org/10.1007/s00603-021-02445-8.

RocScience. (2014). *RocLab 1.0: program for determining rock mass strength parameters. User's manual.* Toronto: RocScience Inc.

Salimi, A., Rostami, J., Moormann, C., & Delisio, A. (2016). Application of non-linear regression analysis and artificial intelligence algorithms for performance prediction of hard rock TBMs. *Tunnelling and Underground Space Technology*, 58, 236-246. https://doi.org/10.1016/j.tust.2016.05.009.

Saroglou, C., Qi, S., Guo, S., & Wu, F. (2018). ARMR, a new classification system for the rating of anisotropic rock masses. *Bulletin of Engineering Geology and the Environment*, 78(5), 3611-3626. https://doi.org/10.1007/s10064-018-1369-4.

Scheldt, T. (2002). *Comparison of continuous and discontinuous modelling for computational rock mechanics* [Doctoral thesis]. Department of Geology and Mineral Resources Engineering, Norwegian University of Science and Technology, Norway.

Serafim, J.L., & Pereira, J.P. (1983) Considerations of the geomechanics classification of Bieniawski. In *Proceedings of the International Symposium on Engineering Geology and Underground Construction*, Lisbon, Portugal.

Somodi, G., Bar, N., Kovács, L., Arrieta, M., Török, Á., & Vásárhelyi, B. (2021). Study of rock mass rating (*RMR*) and geological strength index (GSI) correlations in granite, siltstone, sandstone and quartzite rock masses. *Applied Sciences*, 11(8), 3351. https://doi.org/10.3390/app11083351.

Somodi, G., Krupa, Á., Kovács, L., & Vásárhelyi, B. (2018). Comparison of different calculation methods of Geological Strength Index (GSI) in a specific underground construction site. *Engineering Geology*, 243, 50-58. https://doi.org/10.1016/j.enggeo.2018.06.010.

Stille, H., & Palmström, A. (2008). Ground behaviour and rock mass composition in underground excavations. *Tunnelling and Underground Space Technology*, 23(1), 46-64. https://doi.org/10.1016/j.tust.2006.11.005.

Tokashiki, N., & Aydan, Ö. (2010). The stability assessment of overhanging Ryukyu limestone cliffs with an emphasis on the evaluation of tensile strength of rock mass. *Doboku Gakkai Rombunshuu C*, 66(2), 397-406. https://doi.org/10.2208/jscejc.66.397.

Vučemilović, H. (2022). Technical note calculation of Mohr-Coulomb parameters for rocks of Doha, Qatar. *Geotechnical and Geological Engineering*, 40(3), 1597-1605. https://doi.org/10.1007/s10706-021-01958-x.

Wang, J., Zhang, W., Tan, C., Nie, Z., Ma, W., Chen, D., & Sun, Q. (2023). Multi-dimensional size effects and representative elements for non-persistent fractured rock masses: a perspective of geometric parameter distribution. *Journal of Rock Mechanics and Geotechnical Engineering*, 15(9), 2339-2354. https://doi.org/10.1016/j.jrmge.2022.11.010.

Xing, Y., Kulatilake, P.H.S.W., & Sandbak, L.A. (2017). Rock mass stability investigation around tunnels in an underground mine in USA. *Geotechnical and Geological Engineering*, 35(1), 45-67. https://doi.org/10.1007/s10706-016-0084-9.

Zheng, Z., Zheng, H., Zhao, J., Liu, Z., Feng, G., & Qiu, S. (2023). Ductile-brittle quantitative evaluation of rock based on post-peak properties under true triaxial stress. *Geomechanics and Geophysics for Geo-energy and Geo-resources*, 9(1), 81. https://doi.org/10.1007/s40948-023-00567-7.